engineering proceedings

MDPI

Proceeding Paper

UV-Activated Hybrid Hierarchical ZnO/ZIF-8 Gas Sensor †

Svetlana Nalimova [1,*], Zamir Shomakhov [2], Arina Rybina [1], Sergey Buzovkin [1] and Cong Doan Bui [1]

[1] Department of Micro- and Nanoelectronics, Saint Petersburg Electrotechnical University "LETI", Saint Petersburg 197022, Russia; aarybina@stud.etu.ru (A.R.); ssbuzovkin@stud.etu.ru (S.B.); congdoan6997@mail.ru (C.D.B.)

[2] Institute of Electronics, Robotics and Artificial Intelligence, Kabardino-Balkarian State University named after H.M. Berbekov, Nalchik 360004, Russia; shozamir@yandex.ru

* Correspondence: sskarpova@list.ru

† Presented at the 13th International Electronic Conference on Sensors and Applications, 18–20 November 2026; Available online: https://sciforum.net/event/ECSA-13.

Abstract

Metal–organic frameworks (MOFs) are new crystalline hybrid materials that have aroused great interest because of their growing applications in drug delivery, gas storage, and catalysis. The key limitation of pure MOFs for use in gas sensors is their low conductivity. Therefore, composites are often used. ZIF-8 improves the gas-sensitive characteristics of composites due to its hydrophobic properties, thermal stability, and high specific surface area. The purpose of this study was to design a hierarchical structure of ZnO nanowires coated with a porous ZIF-8 shell and to study its characteristics in detecting volatile organic compounds. ZnO/ZIF-8 composites were synthesized by the solvothermal method and annealed at 320 °C. Scanning electron microscopy revealed a net-like structure on the surface of ZnO nanowires. The gas analytical response was studied at 250 °C under the influence of acetone and ethanol vapors. The response and recovery times for the ZnO/ZIF-8 structure were found to be much longer in the presence of these gases compared to pure zinc oxide nanowires. The additional UV irradiation of ZnO/ZIF-8 provided an increased response and significantly reduced response and recovery times. UV irradiation accelerates the diffusion of gas molecules to the surface of ZnO through the ZIF-8 porous structure. This process leads to faster gas adsorption and desorption. Additional factors are photoinduced charge transfer and water desorption at the ZnO/ZIF-8 interface, contributing to the observed changes in the response.

Keywords: gas sensors; zinc oxide; metal–organic frameworks; hierarchical structure

1. Introduction

Currently, many different types of gas sensors are available, which can be classified into several categories depending on the detection mechanism (mass-sensitive [1], spectral [2], electrochemical [3], chemiresistive [4], and others). Semiconductor gas sensors, which are studied in this paper, attract attention because of their simple operation, the possibility of miniaturization, and their low cost [5]. Semiconductor gas sensors based on metal oxides are widely used for the detection of toxic and explosive gases, air quality control, medical diagnostics (analysis of exhaled air), and in smart home systems [6]. The key requirements for modern sensors are low operating temperature, high sensitivity, and selectivity. However, common sensors based on pure zinc oxide (ZnO) or tin dioxide (SnO_2) often require heating to 300–400 °C, suffer from signal drift, and show cross-sensitivity to water [7]. Therefore, the development of new materials and structures to overcome these limitations is relevant.

Check for updates

Academic Editor: Stefano Mariani

Published: 29 October 2026

Copyright: © 2026 by the authors. Licensee MDPI, Basel, Switzerland. This article is an open access article distributed under the terms and conditions of the Creative Commons Attribution (CC BY) license.

There are several strategies for improving gas-sensitive characteristics. The first is morphological control via the creation of 0D (quantum dots), 1D (nanowires, nanofibers, nanotubes), 2D (nanofilms), 3D (nanoflowers, porous and hollow spheres) structures, as well as hierarchical and porous materials [8]. The second strategy is the formation of heterojunctions when a depleted layer forms at the interface of different semiconductors [9]. The modulation of its width under the influence of gas leads to a sharp change in resistance. The third approach is the functionalization of the surface with noble metal catalysts activating reactions with the target gas [10,11], or with metal–organic frameworks that act as a molecular sieve to increase selectivity [12–15].

Zinc oxide, an n-type semiconductor with a direct band gap (E_g = 3.4 eV), has high electron mobility, thermal stability, and good electrical properties for use in gas-sensitive systems. In addition, this material is attractive because it can be easily produced by chemical synthesis methods in the form of nanowires, nanofibers, nanoflowers, and others [16]. These morphologies can be organized into three different types of crystal structure: NaCl-type structure (obtained at high pressures), sphalerite structure, and wurtzite structure (a hexagonal tightly packed structure with the P63mc spatial group, easily obtained under environmental conditions) [17]. All crystal structures have structural defects of different nature. These defects can affect the properties of grain boundaries, mechanical properties, and electrical conductivity.

Despite the many positive characteristics of ZnO, there are certain disadvantages, including low selectivity, high operating temperatures for activating adsorbed oxygen species, and increased reactivity to the target gas [7]. High temperatures can reduce the stability and exploitation period of the sensor, as well as cause uncontrolled grain growth and limit the detection of explosive gases. The serious disadvantage is the adsorption of water molecules present in the atmosphere, which can interact with ZnO through chemical and physical adsorption processes.

An alternative class of materials is metal–organic frameworks (MOFs), which are porous coordination polymers. Their potential for gas sensors is due to the ability to enhance the adsorption of gases through metal ions and functional groups, as well as the presence of open metal ions serving as active sites for electron transfer. MOFs also have large surface area and adjustable porosity. A key limitation of pure MOFs for gas sensors is low conductivity due to the insulating properties of organic ligands [18]. This complicates direct conversion of a chemical signal into an electrical one. Therefore, MOFs are used as parts of composite materials [19].

Among various MOFs, zeolitic imidazolate frameworks (ZIFs) synthesized from zinc and imidazolate ligands are of particular interest. ZIF-8 is the most thoroughly studied material that can improve the performance of metal oxide gas sensors due to its moisture resistance, thermal stability, and large specific surface area [20]. ZIF-8 can be easily synthesized under mild conditions as uniform and defect-free structures. The most commonly used synthesis methods are solvothermal and mechanochemical approaches [21].

The aim of this work is to synthesize the hybrid hierarchical structures of ZnO nanowires coated with a ZIF-8 shell and study the influence of MOF coating on the gas-sensing performance of these structures.

2. Materials and Methods

2.1. Synthesis of ZnO Nanowires

All reagents were purchased from LenReactiv (St. Petersburg, Russia).

Before growing the nanowires, it was necessary to form a seed layer, a dense layer of small ZnO crystallites that serve as pre-existing nucleation sites for the subsequent growth of the nanowires. Zinc acetate dihydrate ($Zn(CH_3COO)_3{\cdot}2H_2O$, 56 mg) was dissolved

in 50 mL of distilled water in an ultrasonic bath for 5 min. The resulting solution was deposited onto substrates with interdigitated electrodes in three layers via spin coating. The substrates were then annealed in a muffle furnace at 500 °C for 30 min [22].

For the synthesis of the nanowires, a hydrothermal method was used [23,24]. Zinc nitrate hexahydrate ($Zn(NO_3)_2 \cdot 6H_2O$, 148 mg) and hexamethylenetetramine ($C_6H_{12}N_4$, 70 mg) were dissolved in 40 mL of water. The substrates were placed at the bottom of an autoclave and poured with the prepared solution. The synthesis was carried out at 85 °C for one hour. Thereafter, the substrates were rinsed with water, dried at 40 °C, and annealed at 500 °C for 30 min.

2.2. Synthesis of ZnO/ZIF-8 Structure

For the growth of the ZIF-8 structure on zinc oxide nanowires, 2-methylimidazole was used as the precursor. An amount of 200 mg of 2-methylimidazole was mixed with 24 mL of dimethylformamide (DMFA) and 6 mL of deionized water. The resulting solution was transferred into an autoclave, at the bottom of which ZnO nanowire-coated substrates had been placed. The autoclave was maintained at 70 °C for 20 h in a thermostatic oven, then allowed to cool to room temperature. Upon completion of the synthesis, the substrates were rinsed with ethanol and subsequently annealed at 320 °C in a furnace for 1 h.

In this synthesis, the surface of the zinc oxide nanowires serves as the source of Zn^{2+} ions, which are essential for the formation of the ZIF-8 shell.

2.3. Characterization

Scanning electron microscopy (SEM) was used to study the morphology and microstructure of the samples (Tescan VEGA3LMH, Tescan, Czech Republic). The gas-sensing performance of the synthesized structures was evaluated using a laboratory setup (Figure 1). All measurements were carried out under an applied voltage of 5 V. The electrical current was recorded with a Keithley 6485 picoammeter (Keithley, Cleveland, OH, USA). The gas flow was controlled by a computer-operated electromechanical valve, which alternated between two operating modes. In the first mode, the sensing chamber was continuously purged with dry air, whereas in the second mode, a mixture of dry air and the target gas was introduced. The gas flow rates were regulated and monitored using EL-FLOW electronic mass flow meters (Bronkhorst Nederland B.V., Ruurlo, The Netherlands). The concentration of the target gas vapor was calculated based on its saturation vapor pressure at room temperature:

$$C = \frac{P_{gas} F_{gas}}{P_{atm}\left(F_{gas} + F_{air}\right)}, \quad (1)$$

where P_{gas} is the saturated vapor pressure of the target liquid, F_{gas} is the airflow rate passing through the bubbler, P_{atm} is the atmospheric pressure, and F_{air} is the flow rate of the dilution air. The gas-sensing response was evaluated by exposing the samples to acetone, ethanol, and isopropanol vapors.

$$S = \frac{R_{air}}{R_{gas}}, \quad (2)$$

where R_{air} is the resistance of the sensor in the air atmosphere, and R_{gas} is the resistance of the sensor in the atmosphere of the target gas.

Response and recovery times refer to the time it takes for the sensor's resistance to change by 90% after target gas and air have been supplied, respectively.

In Figure 1, dark-red arrowheads on the gas lines indicate the direction of gas flow. Dashed purple arrows indicate the electrical connections between the sensor in the test chamber and the measuring devices, through which the bias voltage $U = 5$ V was applied to the sensor and the current I was measured. The red double-headed arrow indicates data

exchange between the measuring devices and the computer, which was used for instrument control and data acquisition. Mass flow controllers MFC1 and MFC2 set the airflow rate through the bubbler (F_{gas}) and the dilution airflow rate (F_{air}) in Equation (1), respectively.

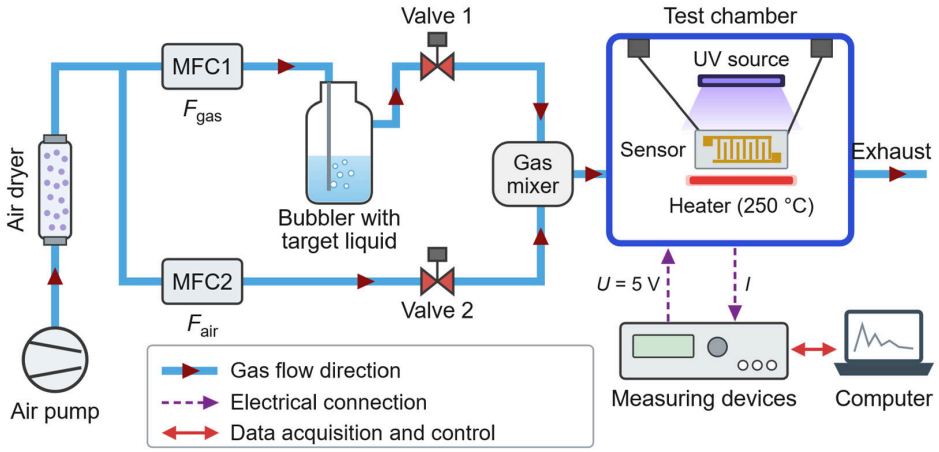
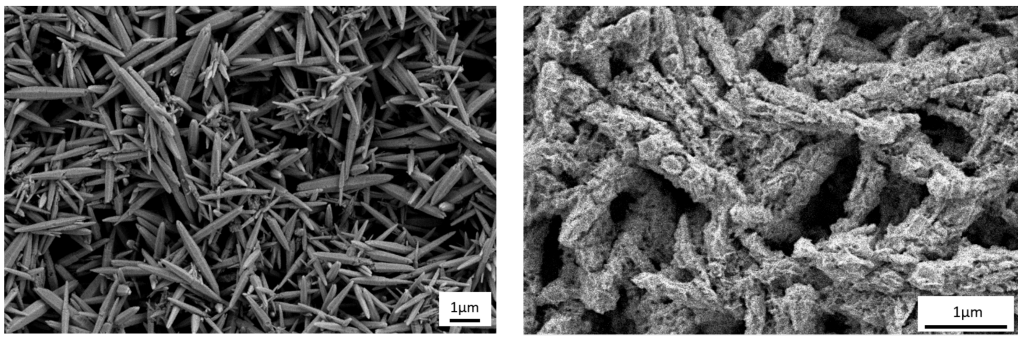


Figure 1. The scheme of the measuring laboratory setup for gas-sensing measurements [25].

3. Results

The samples containing the synthesized zinc oxide nanowires were examined using scanning electron microscopy (SEM). The topographic contrast mode was chosen for the morphological analysis. As shown in Figure 2a, the synthesized nanowires have an average diameter of approximately 130 nm. It can also be observed that the structure consists of an array of nanowires formed through growth from numerous seed nanoparticles.



a **b**

Figure 2. SEM images of zinc oxide nanowires (**a**) and ZnO/ZIF-8 structures (**b**).

The SEM image of ZnO/ZIF-8 structure is shown in Figure 2b. A porous shell can be clearly observed on the surface of the zinc oxide nanowires.

The gas-sensing studies were carried out at a heating temperature of 250 °C and at various concentrations of the supplied gases. The gas sensitivity data are presented and summarized in Table 1.

It can be seen that the response and recovery times became significantly longer after depositing a ZIF-8 shell on the surface of ZnO nanowires. Therefore, the ZnO/ZIF-8 structure was investigated under UV irradiation at a temperature of 250 °C. The results are presented in Table 2.

Comparing the gas-sensing results from Tables 1 and 2, it can be observed that the response increased, while the response and recovery times became significantly shorter. This may be associated with the fact that UV irradiation generates additional electron–hole pairs in ZnO. The holes migrate to the surface and react with chemisorbed oxygen species.

This releases electrons, leading to a significant increase in conductivity. In the presence of a reducing gas, the reaction with photogenerated holes occurs more readily, which enhances the resistance modulation. The influence of UV exposure on the resistance of ZnO/ZIF-8 is shown in Figure 3.

Table 1. Gas-sensing performance results.

Sample	Gas	Concentration, ppm	Response	Response/Recovery Time, s
ZnO	Ethanol	500	1.24	178/413
		1000	1.57	33/256
		1500	2.04	21/216
	Acetone	1000	1.29	270/310
		2000	1.35	226/316
		3000	1.48	217/540
ZnO/ZIF-8	Ethanol	500	2.08	300/492
		1000	2.13	351/558
		1500	2.17	383/676
	Acetone	1000	1.26	218/220
		2000	1.7	689/547
		3000	1.8	848/792

Table 2. Gas-sensing performance of ZnO/ZIF-8 under UV irradiation at 250 °C.

Structure	Gas	Concentration, ppm	Response	Response/Recovery Time, s
ZnO/ZIF-8	Ethanol	500	2	129/200
		1000	2.6	90/298
		1500	2.95	126/300
	Acetone	1000	1.7	129/245
		2000	2.11	131/262
		3000	2.46	109/253

The decrease in response and recovery times may be related to the fact that UV irradiation accelerates the diffusion of gas molecules through the pores of ZIF-8 toward the ZnO surface. In addition, photoinduced charge transfer and water desorption processes may occur at the ZnO/ZIF-8 interface; therefore, the surface becomes more active.

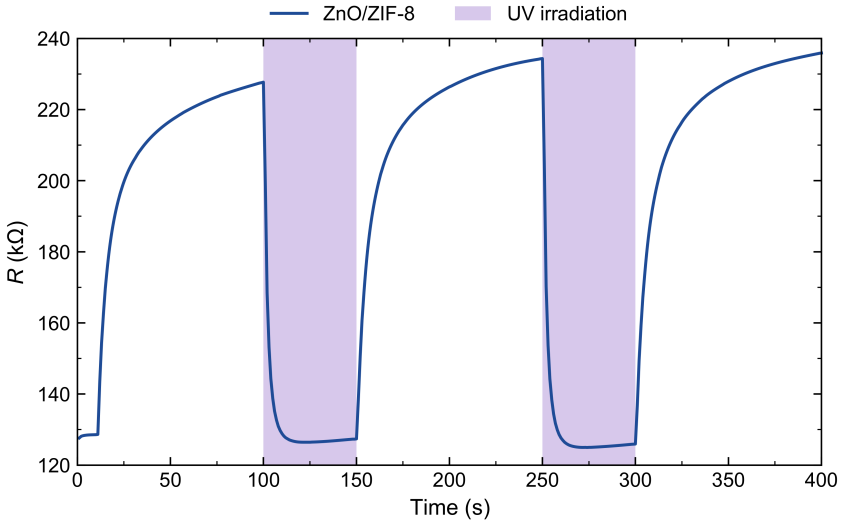


Figure 3. The dependence of ZnO/ZIF-8 resistance on exposure to UV radiation.

4. Conclusions

Modification of ZnO nanowires with the metal–organic framework ZIF-8 using DMFA resulted in the formation of core–shell structures. It was demonstrated that the gas-sensing performance of the ZnO/ZIF-8 composite strongly depends on the synthesis conditions. The best results were achieved using the solvothermal method, where DMFA was used as the solvent. Additional UV irradiation of the ZnO/ZIF-8 structure reduced the response and recovery times and enhanced the sensor response, which is attributed to the photogeneration of electron–hole pairs and the accelerated diffusion of gases through the ZIF-8 pores.

Author Contributions: Conceptualization, S.N. and Z.S.; methodology, S.N. and Z.S.; formal analysis, S.B., A.R., and C.D.B.; investigation, S.B., A.R., and C.D.B.; writing—original draft preparation, S.B. and A.R.; writing—review and editing, S.N., Z.S., and C.D.B.; supervision, S.N. and Z.S. All authors have read and agreed to the published version of the manuscript.

Funding: This research was funded by the Russian Science Foundation, grant number 26-29-20111 (https://rscf.ru/project/26-29-20111/, accessed on 10 June 2026), and the Saint Petersburg Science Foundation, agreement number 26-29-20111 dated 10 June 2026.

Institutional Review Board Statement: Not applicable.

Informed Consent Statement: Not applicable.

Data Availability Statement: Data are contained within the article.

Acknowledgments: During the preparation of this proceeding paper, the authors used ChatGPT (OpenAI, model GPT-6; accessed September 2026) for the purposes of language editing. The authors have reviewed and edited the output and take full responsibility for the content of this publication.

Conflicts of Interest: The authors declare no conflicts of interest.

References

1. Wang, L.; Song, J.; Yu, C. Recent progress on mass-sensitive gas sensors for environmental and industrial applications. *Measurement* **2025**, *249*, 117039. [CrossRef]
2. Hong, Y.; Wei, L.; Zhang, Q.; Deng, Z.; Liao, X.; Zhou, Y.; Wang, L.; Li, T.; Liu, J.; Xiao, W.; et al. A broad-spectrum gas sensor based on correlated two-dimensional electron gas. *Nat. Commun.* **2023**, *14*, 8496. [CrossRef] [PubMed]
3. Wu, Q.; Ding, Z.; Zhang, W. Research progress on electrochemical gas sensors for fire detection. *Int. J. Electrochem. Sci.* **2025**, *20*, 1010. [CrossRef]
4. Luo, S.; Fan, Z.; Ye, Y.; Li, X.; Yang, D. Metal oxide semiconductor-based hydrogen gas sensors: A comprehensive review. *Int. J. Hydrogen Energy* **2026**, *206*, 153405. [CrossRef]
5. Wang, Y.; Zhou, Y.H. Recent Progress on Anti-Humidity Strategies of Chemiresistive Gas Sensors. *Materials* **2022**, *15*, 8728. [CrossRef] [PubMed]
6. Li, G.; Zhu, X.-T.; Liu, J.; Li, S.; Liu, X. Metal Oxide Semiconductor Gas Sensors for Lung Cancer Diagnosis. *Chemosensors* **2023**, *11*, 251. [CrossRef]
7. Chai, H.; Zheng, Z.; Liu, K.; Xu, J.; Wu, K.; Luo, Y.; Liao, H.; Debliquy, M.; Zhang, C. Stability of Metal Oxide Semiconductor Gas Sensors: A Review. *IEEE Sens. J.* **2022**, *22*, 5470–5481. [CrossRef]
8. Mirzaei, A.; Ansari, H.R.; Shahbaz, M.; Kim, J.-Y.; Kim, H.W.; Kim, S.S. Metal Oxide Semiconductor Nanostructure Gas Sensors with Different Morphologies. *Chemosensors* **2022**, *10*, 289. [CrossRef]
9. Giri, S.; Gardner, J.W.; Guha, P.K.; Ghosh, A.; Santra, S. Nanoscale Metal Oxide Heterojunction Chemiresistive Gas Sensor: A Review. *Nano Futur.* **2025**, *9*, 032001. [CrossRef]
10. Chumakova, V.; Marikutsa, A.; Platonov, V.; Khmelevsky, N.; Rumyantseva, M. Distinct Roles of Additives in the Improved Sensitivity to CO of Ag- and Pd-Modified Nanosized $LaFeO_3$. *Chemosensors* **2023**, *11*, 60. [CrossRef]
11. Nalimova, S.S.; Shomakhov, Z.V.; Kozodaev, D.A.; Rybina, A.A.; Buzovkin, S.S.; Bui, C.D.; Moshnikov, V.A. VOC gas sensors based on zinc Stannate nanoparticles decorated with silver. *Nanomaterials* **2024**, *14*, 1993. [CrossRef] [PubMed]
12. Cho, S.R.; Kim, D.-H.; Jeon, M.; Rani, P.; Gyeon, M.; Kim, Y.; Jo, M.; Song, S.; Park, J.Y.; Kim, J.; et al. Overlaying Monolayer Metal–Organic Framework on PtSe2-Based Gas Sensor for Tuning Selectivity. *Adv. Funct. Mater.* **2022**, *32*, 2207265. [CrossRef]

13. Yao, M.-S.; Cao, L.-A.; Tang, Y.-X.; Wang, G.-E.; Liu, R.-H.; Naresh Kumar, P.; Wu, G.-D.; Deng, W.-H.; Hong, W.-J.; Xu, G. Gas transport regulation in a MO/MOF interface for enhanced selective gas detection. *J. Mater. Chem. A* **2019**, *31*, 18397–18403. [CrossRef]
14. Poschmann, M.P.M.; Siebert, L.; Lupan, C.; Lupan, O.I.; Schütt, F.; Adelung, R.; Stock, N. Surface Conversion of ZnO Tetrapods Produces Pinhole-Free ZIF-8 Layers for Selective and Sensitive H2 Sensing Even in Pure Methane. *ACS Appl. Mater. Interfaces* **2023**, *15*, 38674–38681. [CrossRef] [PubMed]
15. Huang, S.; Li, J. Construction of ZnO@ZIF-8 Core–Shell Heterostructure for Enhanced Formaldehyde Selective Performances at Room Temperature. *Appl. Organomet. Chem.* **2025**, *39*, e70166. [CrossRef]
16. Guo, W.; Liu, T.; Zhang, H.; Sun, R.; Chen, Y.; Zeng, W.; Wang, Z. Gas-sensing performance enhancement in ZnO nanostructures by hierarchical morphology. *Sens. Actuators B Chem.* **2012**, *166*, 492–499. [CrossRef]
17. Raha, S.; Ahmaruzzaman, M. ZnO Nanostructured Materials and Their Potential Applications: Progress, Challenges and Perspectives. *Nanoscale Adv.* **2022**, *4*, 1868–1925. [CrossRef] [PubMed]
18. Park, C.; Baek, J.W.; Shin, E.; Kim, I. Two-Dimensional Electrically Conductive Metal–Organic Frameworks as Chemiresistive Sensors. *ACS Nanosci. Au* **2023**, *3*, 353–374. [CrossRef] [PubMed]
19. Wang, S.; Luo, L.; Wu, A.; Wang, D.; Wang, L.; Jiao, Y.; Tian, C. Recent advances in tailoring zeolitic imidazolate frameworks (ZIFs) and their derived materials based on hard template strategy for multifunctional applications. *Coord. Chem. Rev.* **2024**, *498*, 215464. [CrossRef]
20. Paul, A.; Banga, I.K.; Muthukumar, S.; Prasad, S. Engineering the ZIF-8 Pore for Electrochemical Sensor Applications—A Mini Review. *ACS Omega* **2022**, *7*, 26993–27003. [CrossRef] [PubMed]
21. Ahmad, W.; Tahir, M.; Bibi, B.; Gong, F.; He, L.; Tang, H.; Dai, J. Advances in ZIF-8 variants: Synthesis, design, and applications in gas sensing. *Coord. Chem. Rev.* **2025**, *539*, 216733. [CrossRef]
22. Wu, X.; Xiong, S.; Mao, Z.; Hu, S.; Long, X. A designed ZnO@ ZIF-8 core–shell nanorod film as a gas sensor with excellent selectivity for H_2 over CO. *Chem.-Eur. J.* **2017**, *23*, 7969–7975. [CrossRef] [PubMed]
23. Nalimova, S.; Shomakhov, Z.; Bobkov, A.; Moshnikov, V. Sacrificial doping as an approach to controlling the energy properties of adsorption sites in gas-sensitive ZnO nanowires. *Micro* **2023**, *3*, 591–601. [CrossRef]
24. Azmi, Z.H.; Aris, S.N.M.; Abubakar, S.; Sagadevan, S.; Siburian, R.A.F.; Paiman, S.B. Effect of Seed Layer on the Growth of Zinc Oxide Nanowires by Chemical Bath Deposition Method. *Coatings* **2022**, *12*, 474. [CrossRef]
25. Bui, C.D.; Nalimova, S.; Kondratev, V.; Shomakhov, Z.; Kirillova, S.; Maximov, A.; Moshnikov, V. Alcohol Sensing Behavior and Impedance Spectroscopy Characterization of g-C_3N_4 Nanosheets. *Nanomaterials* **2026**, *16*, 213. [CrossRef] [PubMed]

Disclaimer/Publisher's Note: The statements, opinions and data contained in all publications are solely those of the individual author(s) and contributor(s) and not of MDPI and/or the editor(s). MDPI and/or the editor(s) disclaim responsibility for any injury to people or property resulting from any ideas, methods, instructions or products referred to in the content.